Available online at www.sciencedirect.com
SCIENCE DIRECT®
Journal of Non-Crystalline Solids 337 (2004) 174–181
JOURNAL OF NON-CRYSTALLINE SOLIDS
www.elsevier.com/locate/jnoncrysol

Local structure and redox state of copper in tellurite glasses

G.D. Khattak [a], A. Mekki [a], L.E. Wenger [b,*]

[a] Department of Physics, King Fahd University of Petroleum and Minerals, Dhahran 31261, Saudi Arabia
[b] Department of Physics, The University of Alabama at Birmingham, CH 464, 1530, 3rd Avenue S, Birmingham, AL 35294-1170, USA

Received 26 January 2003; received in revised form 18 August 2003
Available online 14 May 2004

Abstract

The local glass structure of tellurite glasses containing CuO with the nominal composition $x(\mathrm{CuO})\cdot(1-x)(\mathrm{TeO_2})$, where $x = 0.10$, 0.20, 0.30, 0.40, and 0.50, as well as the valence state of the copper ions have been investigated by X-ray photoelectron spectroscopy (XPS) and magnetization measurements. The Te 3d core level spectra for all glass samples show symmetrical peaks (Te $3d_{5/2}$ and Te $3d_{3/2}$) at essentially the same binding energies as measured for TeO_2 indicating that the chemical environment of the Te atoms in the glasses does not vary significantly with the addition of CuO. The O 1s spectra, however, show slight asymmetry for all glass samples which results from two contributions, one from the presence of oxygen atoms in the Te–O–Te environment (bridging oxygen BO) and the other from oxygen atoms in an Te–O–Cu environment (non-bridging oxygen NBO). The ratio of NBO to total oxygen was found to increase with CuO content and to be in good agreement with calculated values for the TeO_4 trigonal bipyramid structure. Moreover, the appearance of a satellite peak in the Cu 2p spectra provides definitive evidence for the presence of Cu^{2+} ions in these glass samples where the asymmetry and broadening of the Cu $2p_{3/2}$ and Cu $2p_{1/2}$ peaks are indicative of the presence of both Cu^{2+} and Cu^{+} ions. The relative concentration Cu^{2+} determined from XPS is in good qualitative agreement with the determinations of Cu^{2+} from magnetic susceptibility measurements on the same glass samples. Furthermore the susceptibility data follow a Curie–Weiss temperature-dependent behavior ($\chi = C/(T-\theta)$) with negative Curie temperatures indicating that the predominant magnetic interactions between the Cu^{2+}–Cu^{2+} exchange pairs are antiferromagnetic in nature.

PACS: 61.14.Qp; 61.43.Fs; 75.20.−g

1. Introduction

Tellurium oxide (TeO_2) based glasses are of scientific and technical interest because of their low melting temperatures, high refractive indices, high dielectric constants, and good infrared transmissions, and recently have shown promise for optical fibre or non-linear optical devices applications [1,2]. Since these properties are thought to be due to the anomalous network and electronic structures in the tellurite glasses, numerous structural investigations have been undertaken. Various spectroscopic studies including infrared [3–5], Raman [5–9], nuclear magnetic resonance [10], and X-ray absorption spectroscopy [11–13] as well as X-ray [13,14] and neutron diffraction [15,16] techniques have established that there are two basic structural units, i.e., the TeO_4 trigonal bipyramid (tbp) and the TeO_3 trigonal pyramid, both of which have a lone pair of electrons in one of its equatorial sites.

The addition of transition-metal (TM) oxides to glasses, in general, permits the possibility for the glasses to exhibit semiconducting behavior. This electronic behavior as well as the optical, magnetic, and structural properties for these glasses depends upon the relative ratio of the different valence states of the TM ions present [17–19]. In order to account for the effect of these valence states on these properties of these glasses, it is important to control and measure the ratios of the TM ion concentration in the different valence states of these oxide glasses. X-ray photoelectron spectroscopy (XPS) has proven to be an important and useful technique not only in assessing the local glass structure [20] as it can distinguish between bridging oxygen (BO) and non-bridging oxygen (NBO) [21,22],

* Corresponding author. Tel.: +1-205 934 8659; fax: +1-205 975 6111.
E-mail address: wenger@uab.edu (L.E. Wenger).

0022-3093/$ - see front matter © 2004 Elsevier B.V. All rights reserved.
doi:10.1016/j.jnoncrysol.2003.08.088

but also in estimating the ratio of the different valence states in the TM-oxide glasses [23]. In this study, XPS will be used to investigate the role of Cu in the Cu–tellurite glasses as well as to study the local glass structure. Temperature-dependent magnetic susceptibility measurements combined with inductively coupled plasma spectroscopy (ICP) will provide an independent measure of the relative amounts of the different Cu valence states in these glasses as well as to characterize the nature of any magnetic interaction between the Cu^{2+} ions.

2. Experimental details

2.1. Sample preparation

All glasses were prepared by melting dry mixtures of reagent grade CuO and TeO_2 in alumina crucibles to form nominal $x(CuO)\cdot(1-x)(TeO_2)$ compositions with $x = 0.10$, 0.20, 0.30, 0.40, and 0.50. Since oxidation and reduction reactions in a glass melt are known to depend on the size of the melt, on the sample geometry, on whether the melt is static or stirred, on thermal history, and on quenching rate, all glass samples were prepared under similar conditions to minimize these factors. Approximately 30 g of chemicals were thoroughly mixed in an alumina crucible to obtain a homogenized mixture for each CuO concentration. The crucible containing the nominal mixture was then transferred to an electrically heated melting furnace maintained at 800–850 °C. The melt was left for about an hour under atmospheric conditions in the furnace during which the melt was occasionally stirred with an alumina rod. The homogenized melt was then cast onto a stainless steel plate mold to form glass rods of approximately 5-mm diameter and 2 cm in length for XPS measurements. After casting, the specimens were annealed at 200 °C for 10 h and were stored in a vacuum dessicator to minimize any further oxidation of the glass samples. The actual compositions of the glasses were determined by inductively coupled plasma spectroscopy (ICP) and are listed in Table 1. Although the inclusion of alumina from the crucibles used in the melting of the glass mixtures can be a possible source of impurities, no signals for aluminum were detected in either the XPS or ICP measurements on these glasses.

It should also be noted that attempts to grow glasses with composition $x = 0.6$ did not succeed. For this composition the quenched melt crystallizes and thus compositions of $x \geqslant 0.6$ would be outside the region of glass formation.

Table 1
Nominal and actual composition (molar fraction) of various tellurite glasses containing CuO

Nominal		Actual (from ICP)	
CuO	TeO_2	CuO	TeO_2
0.10	0.90	0.092	0.908
0.20	0.80	0.169	0.831
0.30	0.70	0.272	0.728
0.40	0.60	0.357	0.643
0.50	0.50	0.491	0.509

The relative uncertainty in the ICP results is ±5%.

2.2. XPS measurements

Core level photoelectron spectra were collected on a VG scientific ESCALAB MKII spectrometer equipped with a dual aluminum–magnesium anode X-ray gun and a 150-mm concentric hemispherical analyzer using Al Kα ($h\nu = 1486.6$ eV) radiation from an anode operated at 130 W [24]. Photoelectron spectra of Te 3d, Cu 2p, and O 1s core levels were recorded using a computer-controlled data collection system with the electron analyzer set at a pass-energy of 20 eV for the high-resolution scans. The energy scale of the spectrometer was calibrated using the core level of Cu $2p_{3/2}$ (= 932.67 eV), Cu $3p_{3/2}$ (= 74.9 eV), and Au $4f_{7/2}$ (= 83.98 eV) photoelectron lines. For self-consistency, the C 1s transition at 284.6 eV was used as a reference for all charge shift corrections as this peak arises from hydrocarbon contamination and its binding energy is generally accepted as remaining constant, irrespective of the chemical state of the sample. For XPS measurements, a glass rod from each composition was cleaved in the preparation chamber at a base pressure of 2×10^{-9} mbar before being transferred to the analysis chamber where the pressure was maintained at $<2\times10^{-10}$ mbar.

A non-linear, least-squares algorithm [24] was employed to determine the best fit to each of the O 1s and Cu $2p_{3/2}$ spectra with two Gaussian–Lorentzian curves in order to represent bridging and non-bridging oxygen and two possible copper oxidation states (Cu^{2+} and Cu^{+}), respectively. The fraction of non-bridging oxygen and Cu^{2+} were determined from the respective area ratios from these fits. Based on the reproducibility of similar quantitative spectral decompositions of spectra taken from other surfaces on the same glass samples, uncertainties of ±5% and ±10%, respectively, were estimated for these area ratios. A period of approximately 2 h was required to collect the data set for each sample and there was no evidence of any X-ray induced reduction of the copper in the glasses during this period.

2.3. Magnetic measurements

The temperature-dependent DC magnetic susceptibility was measured using a SQUID magnetometer

(Quantum Design model MPMS-5S) in a magnetic field of 5000 Oe over a temperature range 5–300 K at temperature intervals of 2.5 K. The susceptibility of the sample holder is negligible below 100 K for all samples and constitutes less than a 2% correction at the highest temperature for all samples. The overall accuracy of the magnetic measurements is estimated to be approximately 3% due to the uncertainty of the magnetometer calibration.

3. Results

3.1. Telluride spectra

The high-resolution Te 3d core level spectra for all of the copper–tellurite glasses are collectively displayed in Fig. 1. The doublet peaks attributed to the Te $3d_{5/2}$ and Te $3d_{3/2}$ transitions in these spectra have essentially the same binding energies for all glass samples as well as are in excellent agreement to the corresponding values of 576.1 eV (Te $3d_{5/2}$) and 586.5 eV (Te $3d_{3/2}$) for TeO_2 powder as seen in Table 2. The intensities of the peaks decrease with increasing copper content as expected, while the peaks remain symmetric.

3.2. Oxygen spectra

Fig. 2 shows the O 1s core level spectra for all glasses investigated in this study. While the O 1s peaks are essentially at the same position for all glass samples (see Table 2), the peaks for the $x = 0.30$ and 0.40 samples are considerably broader as evidenced by the larger full-width at half-maximum (FWHM) values. However, upon closer inspection of the O 1 spectra, a slight asymmetry in the O 1s peak is apparent, which would be indicative of two different types of oxygen sites in these glasses. Hence, all O 1s spectra were fitted to two (Gaussian–Lorentzian) peaks in order to determine the peak positions and relative abundance of the different oxygen sites.

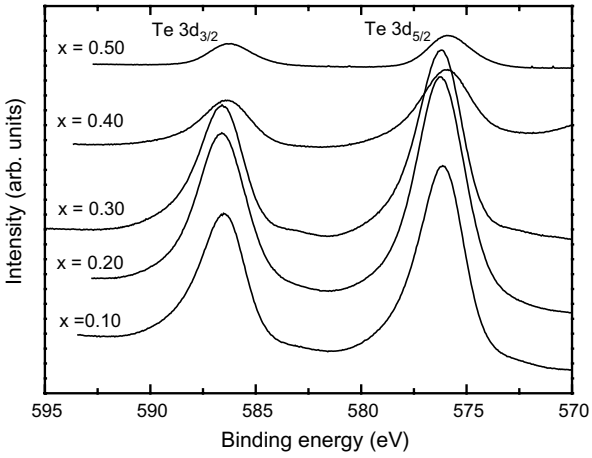

Fig. 1. Core level Te 3d spectra for the $x(CuO)\cdot(1-x)(TeO_2)$ glasses.

3.3. Copper spectra

The Cu 2p spin-orbit doublet spectra for the glasses are shown in Fig. 3. One first notes that the intensities of these Cu 2p peaks grow with increasing CuO content as expected. However, while the locations of the maximum peak intensity for the two spin-orbit components, Cu $2p_{3/2}$ and Cu $2p_{1/2}$, for the $x \leqslant 0.40$ glass samples have binding energies comparable to those measured on CuO powder (see Table 2), the corresponding peaks for the $x = 0.50$ glass sample are approximately 1.5 eV lower. In

Table 2
Peak positions in eV for the core levels Te 3d, Cu 2p, and O 1s relative to C 1s (284.6 eV) and their corresponding FWHM (full-width at half-maximum)

x	Te $3d_{5/2}$ FWHM	Te $3d_{3/2}$ FWHM	ΔE Te 3d	Cu $2p_{3/2}$ FWHM	Cu $2p_{1/2}$ FWHM	ΔE Cu 2p	O 1s FWHM
0.10	576.1 2.64	586.5 2.63	10.4	933.0[a] 3.94	952.6[a] 4.82	19.6	529.8[a] 1.90
0.20	576.2 2.81	586.6 2.79	10.4	933.3[a] 4.00	953.0[a] 4.30	19.7	529.7[a] 2.11
0.30	576.2 2.47	586.6 2.45	10.4	933.4[a] 4.10	953.0[a] 4.60	19.6	529.7[a] 2.44
0.40	575.9 2.36	586.3 2.20	10.4	933.4[a] 3.98	953.4[a] 4.40	20.0	529.7[a] 2.83
0.50	575.9 2.60	586.2 2.62	10.3	932.0[a] 3.34	951.8[a] 3.65	19.8	529.8[a] 1.91
TeO_2	576.1 2.09	586.5 1.96	10.4				530.3 1.93
CuO				933.6 3.31	953.5 3.53	19.9	529.5 1.89

The uncertainty in the peak position is ±0.10 eV and in FWHM is ±0.20 eV.
[a] These peak positions are the average of two peaks.

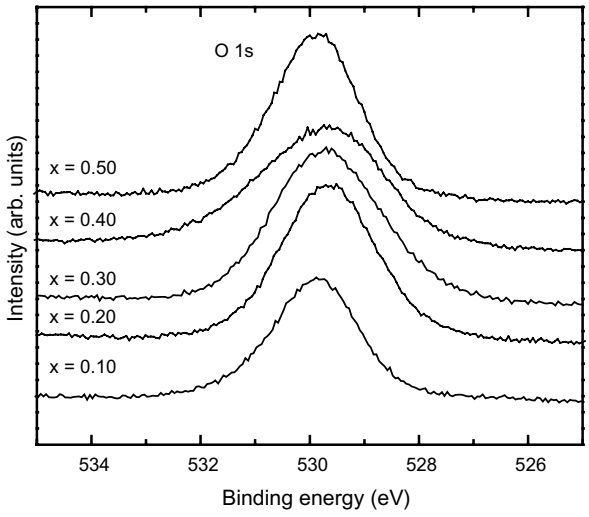

Fig. 2. Core level O 1s spectra for the $x(\mathrm{CuO})\cdot(1-x)(\mathrm{TeO_2})$ glasses.

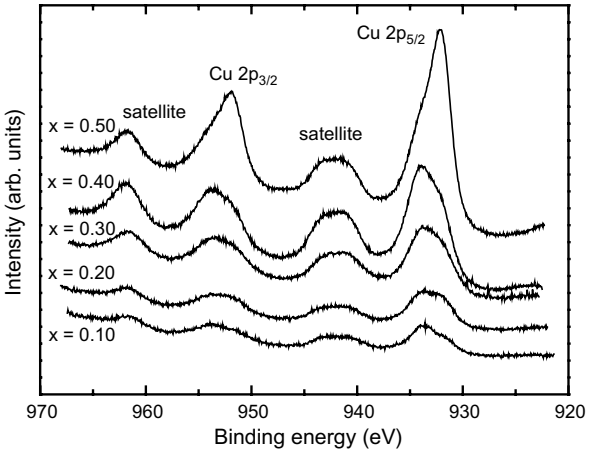

Fig. 3. Core level Cu 2p spectra for the $x(\mathrm{CuO})\cdot(1-x)(\mathrm{TeO_2})$ glasses.

addition, the Cu 2p peaks show significant asymmetry with a shoulder on the lower ($x \leqslant 0.40$ sample) or higher ($x = 0.50$ sample) binding energy side of the main peak. Thus, it is realistic to assume the presence of two separate peaks, one associated with divalent (Cu^{2+}) and the other with monovalent (Cu^{+}) copper ions as these are the only two oxidation states in which Cu can exist in various glasses [25]. Thus the Cu $2p_{3/2}$ spectra for each glass composition were subsequently fitted to two Gaussian–Lorentzian peaks. Lastly, satellite peaks are observed at about 10 eV on the higher binding energy side of both Cu 2p peaks.

3.4. Magnetic susceptibility measurements

The magnetic susceptibility results for these glasses are displayed in Fig. 4 as plots of the magnetic susceptibility, M/H, as a function of the temperature T. The

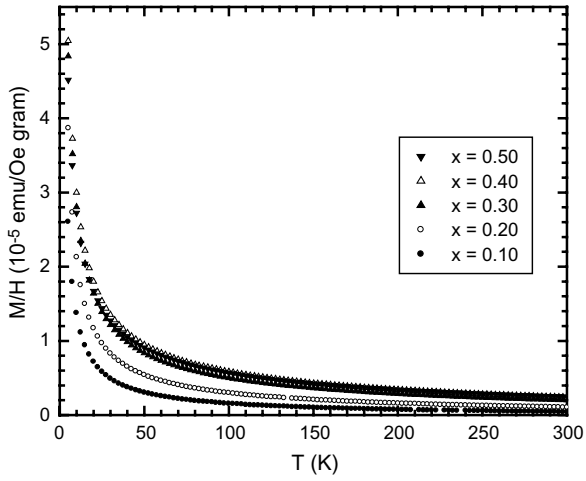

Fig. 4. Magnetic susceptibility versus temperature for the $x(\mathrm{CuO})\cdot(1-x)(\mathrm{TeO_2})$ glasses.

susceptibility data appear to follow a Curie–Weiss behavior ($M/H = C/(T-\theta)$) for all samples except for the sample with $x = 0.10$ where it was found that the data could be satisfactorily fitted to a negative temperature-independent constant plus a Curie temperature-dependent contribution. The temperature-independent constant for this sample was determined from a high-temperature extrapolation of M/H versus $1/T$ plots for temperatures above 200 K. After subtracting these temperature-independent constants from the measured susceptibility data, the resulting $M^*/H(= M/H - (M/H)_{\mathrm{constant}})$ data follow a Curie–Weiss behavior ($M/H = C/(T-\theta)$) as demonstrated in Fig. 5. The resulting parameters $(M/H)_{\mathrm{constant}}$ and the Curie constant C obtained from a least-squares fitting procedure are listed in Table 3 for all samples.

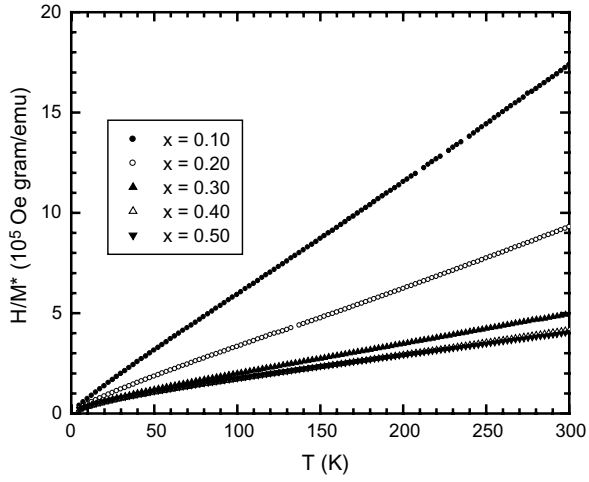

Fig. 5. The inverse of the 'corrected' magnetic susceptibility ($M^*/H = M/H - (M/H)_{\mathrm{constant}}$) as a function of temperature for CuO–tellurite glasses.

Table 3
Magnetic susceptibility results for the copper telluride glasses $(CuO)_x(TeO_2)_{1-x}$ samples and the concentration of Cu^{2+} ions to total copper ions

x	$(M/H)_{constant}$ (10^{-4} emu/Oe g)	C (10^{-7} emu K/Oe g)	θ (K)	$[Cu^{2+}]/[Cu_{total}]$
0.10	−1.6	1.79	−5.58	0.794
0.20	0.0	3.31	−11.4	0.775
0.30	0.0	6.69	−33.1	0.914
0.40	0.0	8.17	−39.8	0.824
0.50	0.0	8.73	−54.1	0.626

4. Discussion

As described in the result section, the doublet peaks attributed to Te $3d_{3/2}$ and Te $3d_{5/2}$ in the Te 3d spectra have essentially the same binding energies and FWHM for all glass samples, although the binding energies for the $x \geqslant 0.40$ glass samples are shifted by ~0.3 eV to lower energies. This shift can be explained in terms of the small difference in the electronegativity of the two cations rather than a change in coordination of the Te from a TeO_4 trigonal bipyramid to a TeO_3 trigonal pyramid glass structure. The smaller electronegativity of Cu (1.90) as compared to that of Te (2.1) should result in a small increase in the electron density at the Te atom with the addition of Cu and correspondingly a small decrease in the Te 3d binding energies, as observed. Moreover, the 0.3 eV shift in the Te 3d binding energies for the most concentrated CuO-containing tellurite glasses is much smaller than the shifts observed in the Te 3d spectra from an earlier XPS study on R_2O–TeO_2 (R: Li, Na, K, Rb and Cs) glasses [26]. Thus it is reasonable to speculate that the local glass structure remains trigonal bipyramid (TeO_4) as the Te atoms are replaced by Cu atoms. Furthermore, the intensities of the peaks decrease with increasing copper content because Te is replaced by Cu and hence there are fewer Te atoms in the sample.

In most XPS studies of oxide glasses, the O 1s spectra are more informative with respect to the structure of the glass than the cation spectra. Specifically, the binding energy of the O 1s electrons is a measure of the extent to which electrons are localized on the oxygen or in the internuclear region, a direct consequence of the nature of the bonding between the oxygen and different cations. As mentioned earlier, a slight asymmetry in the O 1s core level peak is apparent, which indicates two different types of oxygen sites present in these glasses. Most probably, the O 1s peak for the glasses is composed of two peaks corresponding to oxygen atoms in Te–O–Te and Te–O–Cu structural units. The oxygen atoms in Te–O–Te are termed 'bridging' oxygens (BO) while those in Te–O–Cu are 'non-bridging' oxygens (NBO). Moreover, since the BO is covalently bonded to two glass former atoms while the NBO are ionically bonded only from one side, the binding energy of the NBO should be lower than that of the BO. Thus, each O 1s spectrum was deconvoluted into two Gaussian–Lorentzian with the lower binding energy peak corresponding to NBO (Te–O–Cu) and the higher energy peak to BO (Te–O–Te) as shown in Fig. 6 for the $x = 0.20$ and 0.40 glass samples. The resulting peak positions and FWHM for the BO and NBO peaks (see Table 4) are within experimental uncertainties the same for all glass samples and only the relative integrated areas of the peaks change with CuO concentration. Thus the broadness (FWHM) of the O 1s peaks as seen in Fig. 2 and listed in Table 2 is directly

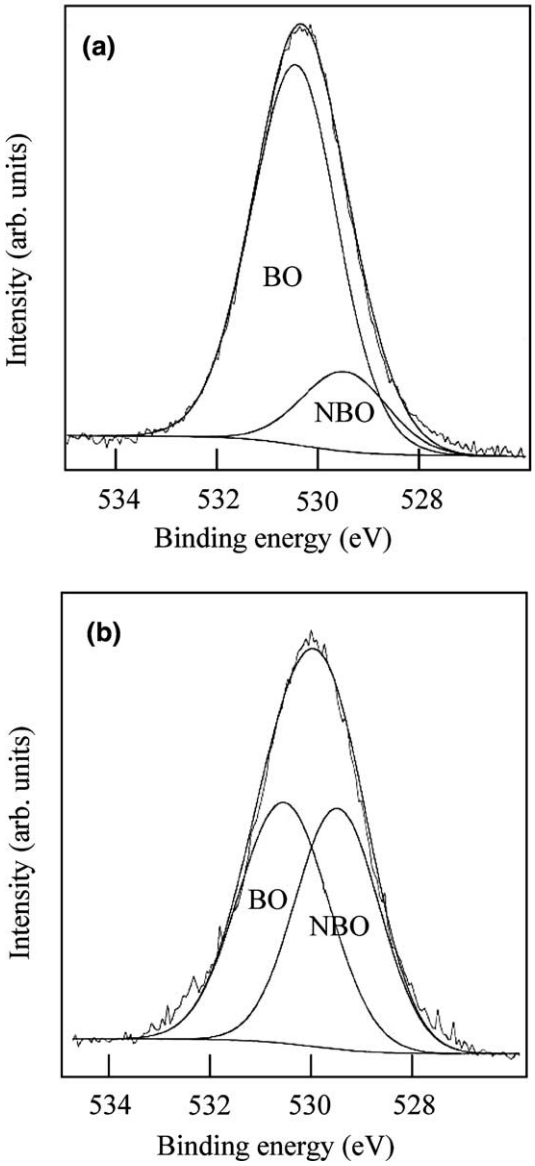

Fig. 6. High-resolution O 1s spectra for the (a) $x = 0.20$ and (b) 0.40 CuO–tellurite glass samples and the resulting NBO and BO peaks (dashed lines) from the least-squares fitting routine of two Gaussian–Lorentzian peaks. The smooth solid line is the resultant sum of the two peaks.

Table 4
Peak positions, FWHM, peak separation, and relative concentration of NBO resulting from the curve fitting of the O 1s core level for the $x\mathrm{CuO}\cdot(1-x)\mathrm{TeO_2}$ glasses

x	O 1s (eV)		FWHM (eV)		$\Delta E_{\mathrm{BO\text{-}NBO}}$ (eV)	[NBO]/[TO]	
	NBO	BO	NBO	BO		Measured	Eq. (1)
0.10	529.1	529.9	1.9	1.9	0.8	0.069	0.096
0.20	529.1	529.9	1.9	2.0	0.8	0.169	0.185
0.30	529.1	529.9	2.1	2.0	0.8	0.304	0.315
0.40	529.2	530.1	1.9	2.0	0.9	0.481	0.435
0.50	529.1	530.1	1.7	1.9	1.0	0.625	0.651

The experimental uncertainty is ±0.2 eV in the energy measurement.

influenced by the relative areas of the BO and NBO peaks as broader spectra will be observed when the areas are comparable, such as for the $x = 0.30$ and 0.40 glass samples. One further notes that the measured area ratio, [NBO/TO], increases roughly linearly with increasing CuO concentration.

The ability to distinguish the BO and NBO peaks in the XPS spectra for this TeO_2 glass system is unlike the earlier XPS study carried out on alkali oxide-tellurite glasses where only a single symmetrical Gaussian–Lorentzian peak was observed from which BO and NBO could not be separated [26] and hence a change in the coordination structure of the tellurium atom was inferred from the Raman spectra. Assuming the copper atoms in the glass behave as network modifiers of the TeO_4 trigonal bipyramid structure (introducing NBO), then each copper oxide molecule will contribute two NBO atoms in the glass [27]. Hence

$$\mathrm{NBO/TO} = 2x/(2-x), \tag{1}$$

where TO represents the total oxygen. The good agreement between the ratios of [NBO/TO] obtained from the above equation and determined from the XPS analysis as shown in Table 4 indicates a consistency with the O 1s peak assignment and that CuO enters the network as a glass modifier without the need to consider the presence of both TeO_4 and TeO_3 structures. In fact, poorer agreement was found between the [NBO/TO] ratio determined from the XPS analysis and that obtained from a model incorporating both TeO structures (see Eq. (7) from Ref. [8]).

As discussed earlier, the peak positions for the two Cu 2p core levels are similar to the peak positions measured in CuO powder for all glass samples except the $x = 0.50$ sample, where a shift of about 1.5 eV to lower energies is found. This shift in binding energy cannot only result from a change in the molecular environment but also from a reduction in the formal oxidation state of the transition metal ion [29]. Indeed the asymmetry observed in the Cu 2p spectra is an indication of the presence of two different valence states for the copper ions in these tellurite glasses. It is well known that copper compounds containing Cu^{2+} have strong satellite peaks while compounds with just Cu^{+} have no satellites [28,29]. Hence the appearance of the satellite peaks at about 10 eV on the higher binding energy side of the main Cu 2p peaks provides definitive evidence for the presence of Cu^{2+} ions in these glass samples. Since the only other oxidation state of copper is Cu^{+}, the Cu $2p_{3/2}$ spectrum was fitted to Gaussian–Lorentzian peaks similar to the fitting procedure used for the O 1s spectra, as shown in Fig. 7 for the $x = 0.20$ and 0.40 samples. (One should note that the satellite peaks are fitted to two curves as well in order to accurately determine the area under the satellite peak and thus do not represent a separate contribution from Cu^{+}.) The corresponding peak positions and FWHM determined from the fitting procedures are listed in Table 5. One further notes that the peak position and FWHM values for both the Cu^{2+} and Cu^{+} are essentially unchanged for each glass sample. This independence of peak position and FWHM values on CuO content is consistent with a reduction of the formal oxidation state of the Cu ion being primarily responsible for any observed binding energy shift in the Cu 2p spectra as a shift would just result from a change in the relative abundance of the two Cu ions. As previously reported [30] the areas under these peaks plus the area under the satellite peak can be used to determine the ratio of Cu^{2+} ions to total Cu ions present. Defining $A1 =$ area under Cu^{+} peak which is proportional to the concentration of Cu^{+}, $A2 =$ sum of areas under Cu^{2+} peak and satellite peaks which is proportional to the concentration of Cu^{2+}, then

$$\mathrm{Cu^{2+}/Cu_{total}} = A2/(A1 + A2). \tag{2}$$

The corresponding ratios determined from these relative areas are reported in Table 5. From these ratios, it is apparent that copper ions exist predominately (>70%) in the Cu^{2+} state for all the Cu–tellurite glasses except for $x = 0.50$ glass where only 44% of the copper ions are in the Cu^{2+} state. Since Cu^{+} is more prevalent in the $x = 0.50$ sample, a shift in the Cu 2p peak to lower energies can be anticipated in agreement with the observed spectra.

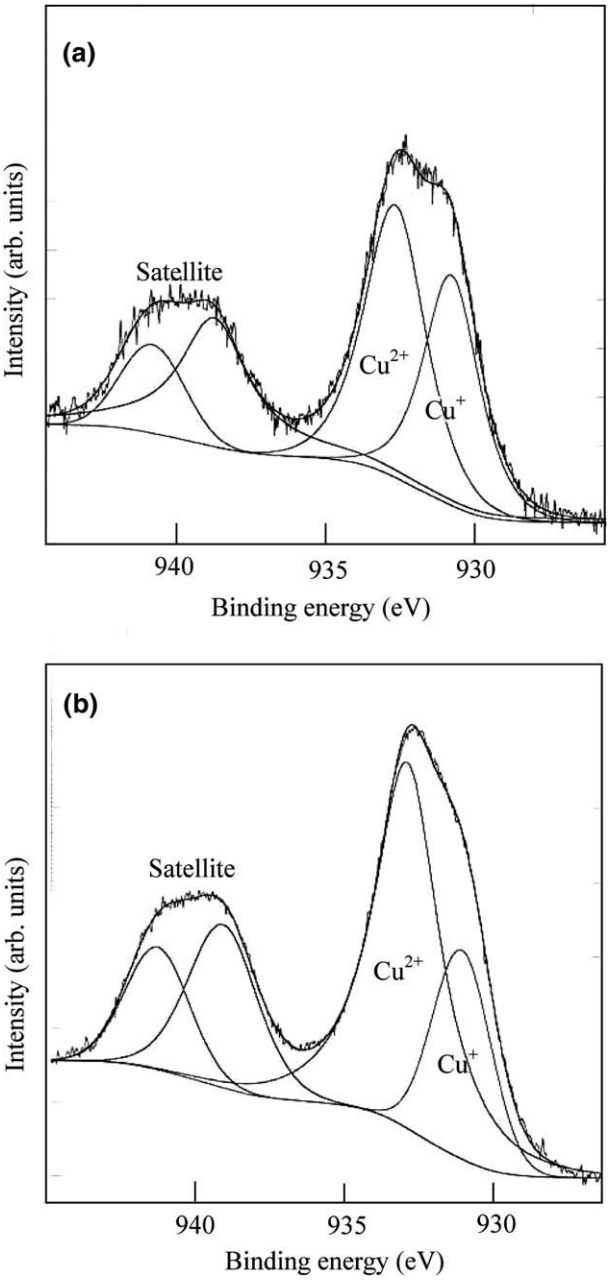

Fig. 7. High-resolution Cu $2p_{3/2}$ spectra for the (a) $x = 0.20$ and (b) 0.40 CuO–tellurite glass samples and the resulting Cu^{2+} and Cu^{+} peaks (dashed lines) from the least-squares fitting routine. The smooth solid line is the resultant sum of the two peaks. The satellite peak associated with Cu^{2+} has been fitted to two curves in order to accurately calculate the area under the peak.

The magnetic susceptibility data supports the conclusion of the XPS studies, i.e., the existence of both magnetic (Cu^{2+}) and non-magnetic (Cu^{+}) copper ions. The ratios of Cu^{2+}/Cu_{total} (see Table 3) determined from the Curie constant, C, in conjunction with the copper concentration determined by ICP show a similar pattern to the XPS results in that the copper ions are predominately in the Cu^{2+} valence state and that the Cu^{2+}/Cu_{total} ratio decreases significantly for the $x = 0.50$ sample from the ratios determined for the other samples. Quantitatively, the two determinations of the ratios are within the experimental uncertainty for all samples except for the $x = 0.50$ sample. This is not too surprising since the magnetic susceptibility is measured on bulk samples while XPS studies just the surface of the glass sample. Also the observation that the magnetic susceptibility follows a Curie–Weiss behavior over the entire measured temperature range indicates that the Cu^{2+} ions behave paramagnetically in the host glass network with only weak interactions between the magnetic ions. The negative sign of the paramagnetic Curie temperature, θ, indicates that the Cu^{2+}–Cu^{2+} interaction is predominately antiferromagnetic in these Cu–tellurite glasses, probably through a superexchange mechanism via the neighboring oxygen atoms. The increasing values of the Curie temperature with increasing copper content reflect not only the increase in the total number of magnetic Cu^{2+} ions present with increasing Cu content, but also an increase in the relative strength of the Cu^{2+}–Cu^{2+} interaction.

5. Conclusions

The binding energies associated with the Te 3d and O 1s core levels for the Cu–tellurite glasses indicate that the local glass structure is similar to that of the TeO_2 glass former as essentially no energy shifts are found for these core levels. The asymmetry found in the Cu $2p_{3/2}$ peak in combination with the presence of a satellite peak approximately 10 eV higher in energy provides evidence for the presence of Cu ions being in the Cu^{2+} oxidation state as well as in the Cu^{+} state. By decomposing the Cu $2p_{3/2}$ into two distinct Gaussian–Lorentzian peaks separated by ~2.1 eV with the higher energy peak being associated with Cu^{2+}, the relative concentration of the two Cu ions is determined from the relative areas under these peaks and the satellite peaks. The Cu^{2+} content is found to be more than 70% for the glasses with $x \leqslant 0.40$ and only 44% for the $x = 0.50$ glass. These findings are in reasonable agreement with those determined from magnetic susceptibility measurements combined with ICP results. Furthermore the Curie–Weiss behavior, $\chi = C/(T - \theta)$, with negative Curie temperatures indicates that the predominate magnetic interactions between the Cu^{2+} ions are antiferromagnetic in nature. The O 1s spectra for all glasses show slight asymmetry and are analyzed in terms of two contributions, one from bridging oxygen (BO) and the other from non-bridging oxygen (NBO). The ratio NBO/TO evaluated for each glass sample is found to be in good agreement with the theoretical values assuming CuO enters the glass network as a glass modifier of the TeO_4 trigonal bipyramid structure with negligible TeO_3 structural units being formed.

Table 5
Peak positions, FWHM, peak separation, and relative concentration of Cu^{2+} resulting from the curve fittings of the Cu $2p_{3/2}$ peaks for the $xCuO\cdot(1-x)TeO_2$ glasses

x	Cu $2p_{3/2}$ (1)			Cu $2p_{3/2}$ (2)			ΔE (eV)	Cu $2p_{3/2}$ (sat) / Area	$[Cu^{2+}]/[Cu_{total}]$ Eq. (2)
	Position	FWHM	Area	Position	FWHM	Area			
0.10	931.5	2.53	2741	933.6	2.80	8071	2.1	5502	0.832
0.20	931.5	2.53	6670	933.5	2.80	8748	2.0	7526	0.709
0.30	931.9	2.53	7586	934.0	3.20	20 952	2.1	13 585	0.820
0.40	931.9	2.53	15 218	933.8	2.90	35 273	1.9	24 582	0.797
0.50	931.9	2.40	42 882	933.9	2.90	19 189	2.0	15 132	0.444

The experimental uncertainty is ±0.1 eV in the energy measurement and ±10% in the relative concentration of Cu^{2+}.

Acknowledgements

Two of the authors (G.D.K. and A.M.) would like to acknowledge the support of KFUPM Research Committee and the Physics Department at KFUPM.

References

[1] J.S. Wang, E.M. Vogel, E. Snitzer, Opt. Mater. 3 (1994) 187.
[2] S.H. Kim, T. Yoko, S. Sakka, J. Am. Ceram. Soc. 76 (1993) 865.
[3] N. Uchida, K. Takahashi, K. Nakata, S. Shibusawa, Yogyo Kyokai Shi 86 (1978) 317.
[4] T. Yoko, K. Kamiya, K. Tanaka, H. Yamada, S. Sakka, Nippon Seramikkusu Kyokai Gakujutsu Ronbunshi 97 (1989) 289.
[5] J. Heo, D. Lam, G.H. Sigel Jr., E.A. Mendoza, D.A. Hensley, J. Am. Ceram. Soc. 75 (1992) 277.
[6] T. Sekiya, N. Michida, A. Ohtsuka, M. Tonokawa, Nippon Seramikkusu Kyokai Gakujutsu Ronbunshi 97 (1989) 1435.
[7] T. Sekiya, N. Michida, A. Ohtsuka, M. Tonokawa, J. Non-Cryst. Solids 144 (1992) 128.
[8] Y. Himei, A. Osaka, T. Nanba, Y. Miura, J. Non-Cryst. Solids 177 (1994) 164.
[9] M. Tastumisago, T. Minami, Y. Kowada, H. Adachi, Phys. Chem. Glasses 35 (1994) 89.
[10] T. Yoko, M. Fujita, F. Miyaji, S. Sakka, Chem. Exp. 5 (1990) 549.
[11] A. Osaka, Q. Jianrong, T. Nanba, Y. Miura, T. Yao, J. Non-Cryst. Solids 142 (1992) 81.
[12] H. Yamamoto, H. Nasu, J. Matsuoka, K. Kamiya, J. Non-Cryst. Solids 170 (1994) 87.
[13] Y. Shimizugawa, T. Maeseto, S. Suehara, S. Inoue, A. Nukui, J. Mater. Res. 10 (1995) 405.
[14] G.W. Brady, J. Chem. Phys. 27 (1957) 300.
[15] S. Neov, V. Kozhukharov, I. Gerasimova, K. Krezhov, B. Sidzhimov, J. Phys. C: Solid State Phys. 12 (1979) 2475.
[16] K. Suzuki, J. Non-Cryst. Solids 95&96 (1987) 15.
[17] M. Sayer, A. Mansingh, Phys. Rev. B 6 (1972) 4629.
[18] G.S. Linsley, A.E. Owen, F.M. Hyayatee, J. Non-Cryst. Solids 4 (1970) 208.
[19] G.W. Anderson, F.U. Luehrs, J. Appl. Phys. 39 (1968) 1634.
[20] C.G. Pantano, in: R. Rew (Ed.), Experimental Techniques of Glass Science, American Ceramic Society, Westerville, OH, 1993, p. 129.
[21] B.M.J. Smets, T.P.A. Lommen, J. Non-Cryst. Solids 46 (1981) 21.
[22] B.M.J. Smets, D.M. Krol, Phys. Chem. Glasses 25 (1984) 113.
[23] G.D. Khattak, M.A. Salim, L.E. Wenger, A.H. Gilani, J. Non-Cryst. Solids 262 (2000) 66.
[24] E.E. Khawaja, Z. Hussain, M.S. Jazzar, O.B. Dabbousi, J. Non-Cryst. Solids 93 (1987) 45.
[25] C.R. Bamford, in: Color Generation and Control in Glass, Elsevier, Amsterdam, 1977.
[26] Y. Himei, Y. Miura, T. Nanba, A. Osaka, J. Non-Cryst. Solids 211 (1997) 64.
[27] A. Mekki, D. Holland, C.F. McConville, J. Non-Cryst. Solids 215 (1997) 271.
[28] G.A. Vernon, G. Stucky, T.A. Carlson, Inorg. Chem. 15 (1976) 278.
[29] G. van der Laan, C. Westra, C. Hass, G.A. Smatzky, Phys. Rev. B 23 (1981) 4369.
[30] G.D. Khattak, M.A. Salim, L.E. Wenger, A.H. Gilani, J. Non-Cryst. Solids 262 (2000) 66.